HHS Public Access

Author manuscript

Microsc Res Tech. Author manuscript; available in PMC 2015 December 10.

Published in final edited form as:

Microsc Res Tech. 2015 March ; 78(3): 195–199. doi:10.1002/jemt.22463.

Laser-Induced Shockwave Paired with FRET: A Method to Study Cell Signaling

VERONICA GOMEZ-GODINEZ[1], **DARYL PREECE**[2], **LINDA SHI**[1], **NIMA KHATIBZADEH**[3], **DERRICK ROSALES**[1], **YIJIA PAN**[1], **LIE LEI**[1], **YINGXIAO WANG**[1,4], and **MICHAEL W. BERNS**[1,3,4,*]

[1]Institute of Engineering in Medicine, University of California, San Diego 9500, Gilman Drive La Jolla, California 92093-0435

[2]Department of NanoEngineering, University of California, San Diego 9500, Gilman Drive La Jolla, California 92093-0448

[3]Beckman Laser Institute and Medical Clinic, 1002 Health Sciences Road East, Irvine, California 92612

[4]Department of Bioengineering, University of California, 9500 Gilman Drive La Jolla, California 92093-0412

Abstract

Cells within the body are subject to various forces; however, the details concerning the way in which cells respond to mechanical stimuli are not well understood. We demonstrate that laser-induced shockwaves (LIS) combined with biosensors based on fluorescence resonance energy transfer (FRET) is a promising new approach to study biological processes in single live cells. As "proof-of-concept," using a FRET biosensor, we show that in response to LIS, cells release intracellular calcium. With the parameters used, cells retain their morphology and remain viable. LIS combined with FRET permits observation of the cells immediate response to a sudden shear force.

Keywords

Calcium; FRET; laser-induced shockwave

INTRODUCTION

We describe the use of fluorescence resonance energy transfer (FRET) to monitor the intracellular change in calcium following exposure to laser-induced shockwaves (LIS). The advantage of utilizing FRET biosensors is that they can be genetically modified to specifically target regions and/or organelles within the cell. Furthermore, high background signals from unbound dye in the extracellular space are greatly reduced, if not eliminated

*Correspondence to: Michael W. Berns, Institute of Engineering in Medicine, University of California, San Diego 9500, Gilman Drive La Jolla, California 92093-0435, United States. E-mail: mwberns@uci.edu.

REVIEW EDITOR: Peter Saggau

entirely (Palmer and Tsien, 2006). LIS has been studied extensively for a range of functions (Lokhandwalla et al., 2001; Reichel et al., 1987; Tao et al., 1987; Vogel et al., 1986). These shock-waves (SWs) are initiated due to the sudden build up of energy at the focus of a pulsed laser beam. The subsequent microplasma—cavitation, followed by expansion and contraction of a short-lived microbubble, can exert large mechanical forces in the surrounding environment. Such SWs induce a sudden shear stress against cells in the vicinity of the microbubble (Compton et al., 2014; Rau et al., 2006). Other studies have investigated the spatio-temporal dynamics of shockwaves (Vogel et al., 1989). In the present study, we focus on the biological application rather than temporal dynamics of LIS.

The combination of LIS and FRET facilitates the study of the subsequent biological process with high temporal and spatial resolution. As “proof-of-concept,” we demonstrate the ability to follow calcium dynamics by FRET following LIS. Previous studies have shown that shear stress is capable of causing an increase of intracellular calcium. However, in these studies, shear stress was applied to all of the cells in a substrate (Liu et al., 2011; Ravin et al., 2012). LIS permits selection of the initiation point of the shockwave, the individual cells to be affected by the resulting shear stress, and the magnitude of the shear stress as a function of the distance of the cell from the shockwave initiation point.

MATERIALS AND METHODS

Laser Setup

The optical setup is described in Figure 1A. The ablation laser is a Coherent Flare 532 nm 100 Hz repetition rate system with a 2 ns pulse width and 450 μJ pulse energy (Spectra-Physics, Mountain View, CA). A mechanical shutter (Vincent Associates, Rochester, NY) with a 10–15 ms duty cycle is gated to allow 1–2 pulses to enter the microscope. A dual-axis fast scanning mirror (FSM-200-01, Newport Corp, Fountain Valley, CA) is used to steer the laser beam in the sample plane.

Cell Culture

Bovine arterial endothelial cells (BAEC) were cultured using Advanced DMEM (Invitrogen, Carlsbad, CA) supplemented with 20% fetal bovine serum and 1% Glutamax. Transient transfections with D3CPV calcium biosensor plasmid were done utilizing Lipofectamine 2000M (Invitrogen, Carlsbad). Upon calcium binding, the D3CPV changed conformation bringing together the blue-fluorescence donor (ECFP) and yellow-fluorescence acceptor (YPet), leading to a decrease in ECFP (blue) fluorescence and an increase in YPet FRET (yellow) fluorescence (Ouyang et al., 2008). The result was a decrease in the ECFP/YPet FRET ratio.

One day after transfection cells were seeded on No. 1.5 glass-bottom imaging dishes (Cell E&G, Houston) coated with 200 μl of 40 μg/mL fibronectin in molecular grade water and allowed to dry before cell seeding. Thirty minutes prior to SW, cells were switched to Hanks buffered saline solution (HBSS) with or without calcium and magnesium (Invitrogen, Carlsbad, CA). Cells were placed on a microscope heating stage (Warner Instruments,

Hamden, CT) at 37°C. Fluorescence measurements were taken in the center of each cell and normalized by dividing post-shockwave ratios by the average of the pre-shockwave ratios.

Propidium Iodide Exclusion

Cells were incubated with 1 μg/mL of propidium iodide (PI) in HBSS and subjected to SW at varying distances to discriminate dying and necrotic cells from live cells. Cells were followed by time-lapse phase contrast imaging in order to assess changes in morphology indicative of delayed SW damage.

Imaging Acquisition and Analysis

Images were acquired on a Zeiss Axiovert 200M microscope (Carl Zeiss, Thornwood, NY) equipped with a 440DF20 excitation filter, a 455DRLP dichroic mirror, and two emission filters (480DF30 for CFP and 535DF25 for YFP). Images were taken every 20 seconds to establish pre-shockwave FRET signals. Post-shockwave images were taken at an interval of 3 seconds for one minute to capture immediate calcium changes. This was followed by an interval of 10 sec onds until cells had been observed for a total of 300 seconds post-LIS. FRET analysis was carried out using the MatLab application, FluoCell (Lu et al., 2011; Lu et al., 2008).

RESULTS

Shockwave Conditions for Cellular Experiments

In order to establish an indication of the effective laser pulse power (and irradiance) in the focal spot, a calibration was performed with 5μm beads in HBSS. The lowest power causing displacement of a bead through the medium is 114–160 μW ($2.95–4.01 \times 10^{12}$ W/cm^2) at the beam focal point. This is consistent with the method used previously (Rau et al., 2006)

A montage of images demonstrates the instantaneous effect of the cavitation bubble that leads to the shockwave. As the distance from LIS increases the shear forces which are a function of the fluid velocity drops off (Fig. 1B). The time-averaged shear stress is greater than 0.1 Pa over a period of 55 μs. However, this is not reflective of the peak shear stress that is likely to be at least 200 times greater. As laser power is increased, the fluid velocity and shear stress increases. Over the range of powers tested, the shear stress was found to increase almost linearly with power.

Cell viability following plasma generation in the irradiance range used ($2.95–8.7 \times 10^{12}$ W/cm^2) was assessed by determination of PI exclusion (none entered the cells at the irradiances and distance from the laser spot used), and phase contrast imaging of the cell morphology for up to 10 minutes following shock wave exposure (Figs. 2A–2C). Cells retained the same morphology as pre-shockwave; there was no cytoplasmic blebbing indicative of the cell lifting off the substrate, no vacuoles formed in the cytoplasm, and the nucleus did not change (i.e., become dark or pycnotic).

When cells were exposed to higher laser powers ranging from 400 μW to 4 mW in the focused spot ($10.8–108 \times 10^{12}$ W/cm^2) immediate cell death and/or shifting of the cell on the glass surface were observed (data not shown). This occurred when the cells were at a

distance of 50–100 μm from the laser focal point (N = 14). Both of these effects are undesirable for FRET as the quantification of intracellular calcium becomes difficult within the same location of the cell if the cell has moved, changed shape or, in fact, died. Consequently, FRET experiments were conducted in the laser irradiance range of 2.95–4.01 × 10^{12} W/cm^2. Figure 2D is an image of cells prior to shockwave. Ten seconds after the shockwave induced with a focal point power of 1.6 mW (43.5 × 10^{12} W/$cm^{2)}$, the cells have detached from the substrate (Fig. 2E, scale bar = 10 um). The perimeters of the cells have been outlined to indicate their location prior to shockwave (Fig. 2E, scale bar = 10 μm). At this, irradiance even cells whose edge is 70 um from the shockwave are affected (refer bottom left Figs. 2D and 2E). In comparison, a cell, the same distance from a SW induced at the lower irradiance, does not display any morphological changes (Fig. 2A–2C).

LIS and FRET: Intracellular Calcium Release

BAEC cells expressing the calcium FRET biosensor, D3CPV, were exposed to LIS at irradiances of 2.95–4.01 × 10^{12} W/cm^2 as described above. Cells in HBSS with and without calcium released calcium into the cytoplasmic space causing FRET ratios to decrease 3 seconds after the shockwave. Ratio and calcium levels are inversely related. Figure 3A is a graph of the nor-malized FRET ratios. Laser shockwave induction was set to T = 0 seconds. An inset shows a magnified view of the FRET ratios up to 30 seconds post-laser (Fig. 3A, N = 5 per condition). FRET in the calcium-free HBSS demonstrated that the observed changes in intracellular calcium originated from internally bound (sequestered) calcium. The calcium concentration of these cells returned to pre-shockwave levels at approximately 80 seconds post-shockwave and continued to decrease beyond pre-shockwave levels (Fig. 3A, red graph).

Figure 3B is a montage of ratiometric images to illustrate the calcium changes with respect to the whole cell. The pixel colors correspond to the fluorescence ratio. Approximately, 36 seconds after SW exposure, the FRET ratio has returned to near initial values in the majority of the cell.

In the presence of HBSS with calcium (Fig. 3A, black graph), intracellular calcium increases immediately after the shockwave and starts to decrease after approximately 30 seconds.

DISCUSSION

We demonstrate the combination of LIS and FRET as a new method to study cell signaling. The impact of the shockwave can be controlled by varying the position from the target cell and/or by varying the laser irradiance in the focal spot.

In this proof-of-concept study, intracellular calcium is released in response to a mechanical stimulus—the shockwave. We identify parameters for shockwave induction that preserve cellular morphology and function. Cells exposed to a shockwave generated by 2.95–4.01 × 10^{12} W/cm^2 do not exhibit visible morphological deformation (compare Figs. 2A to C) and appear structurally unaffected in the FRET images (Fig. 3B). With the laser power and distance parameters used, cells remain viable via time-lapse microscopy and PI exclusion. Therefore, we are able to attribute the internal release of calcium to the shockwave.

Cells in calcium-free medium are able to return to low preshockwave levels and continue to exhibit a decrease in cytoplasmic calcium. This suggests that the mechanical shock wave stimulated the release of calcium from organelles (likely mitochondria and/or other cytoplasmic structures) into the intracellular cytosol. It is also likely that the SW, triggered activation of calcium pumps on the plasma membrane, resulting in a net calcium efflux from the cell. Cells in HBSS with calcium, also attempt to bring calcium levels down. However, the calcium levels remain higher than preshockwave levels suggesting some calcium influx.

In future studies, genetically modified D3CPV can be developed for the purpose of identifying the origin of the calcium by fusing it to a specific protein or by the addition of a localization sequence to the biosensor. Combining FRET and LIS will permit (a) investigation of the signaling molecules responsible for triggering the calcium release, and (b) identification of the precise sources of the released intracellular calcium.

The relationship between cytoplasmic calcium release and laser parameters also requires further investigation. Previous studies showed that the level of cytoplasmic calcium increase depends on the amount of shear stress applied (Liu et al., 2011). It is likely that irradiances higher than 4.0×10^{12} W/cm^2 will cause greater cytoplasmic calcium increases, or that cells further than 100 μm from the initiation site will show less change in cytoplasmic calcium.

In this initial FRET study, only the irradiance range of $2.95–4.0 \times 10^{12}$ W/cm^2 was used. A benefit of utilizing LIS is that the distance of the cell from the shock-wave can be controlled. Thus, major structural alterations to the cytoskeleton and to focal adhesion sights are minimized. Future experiments that couple LIS and FRET biosensors specific for cytoskeleton and molecular motors will permit precise spatial and temporal analysis of shockwave pressure-effects on cytoskeletal dynamics.

In conclusion, the spatial and molecular specificity of FRET biosensors in combination with LIS should be a powerful tool for elucidating the mechanisms of shockwave effects on cells and their organelles and should have significant applications in other areas of cell signaling. In addition, LIS and FRET could be applied to models involving damage and repair of neurons resulting from traumatic pressure-induced injury.

Acknowledgments

This study was supported by a gift from the Beckman Laser Institute Foundation, AFOSR FA9550-08-1-0284 (M.W.B.) and NIH HL09 8472, NIH RO1HL121365, HL109142, NSF CBET 0846429 (Y.W.)

Contract grant sponsor: AFOSR; Contract grant number: FA9550-08-1-0384; Contract grant sponsor: Beckman Laser Institute Foundation; Contract grant numbers: NIH HL098472, NIH RO1HL121365, HL109142, NSF CBET 0846429.

References

Compton JL, Luo JC, Ma H, Botvinick E, Venugopalan V. High-throughput optical screening of cellular mechanotransduction. Nat Photonics. 2014; 8:710–715. [PubMed: 25309621]

Liu B, Lu S, Zheng S, Jiang Z, Wang Y. Two distinct phases of calcium signalling under flow. Cardiovasc Res. 2011; 91:124–133. [PubMed: 21285296]

Lokhandwalla M, McAteer JA, Williams JC Jr, Sturtevant B. Mechanical haemolysis in shock wave lithotripsy (SWL): II. In vitro cell lysis due to shear. Phys Med Biol. 2001; 46:1245–1264. [PubMed: 11324963]

Lu S, Kim TJ, Chen CE, Ouyang M, Seong J, Liao X, Wang Y. Computational analysis of the spatiotemporal coordination of polarized PI3K and Rac1 activities in micro-patterned live cells. PLoS One. 2011; 6:e21293. [PubMed: 21738630]

Lu S, Ouyang M, Seong J, Zhang J, Chien S, Wang Y. The spatiotemporal pattern of Src activation at lipid rafts revealed by diffusion-corrected FRET imaging. PLoS Comput Biol. 2008; 4:e1000127. [PubMed: 18711637]

Ouyang M, Sun J, Chien S, Wang Y. Determination of hierarchical relationship of Src and Rac at subcellular locations with FRET biosensors. Proc Natl Acad Sci U S A. 2008; 105:14353–14358. [PubMed: 18799748]

Palmer AE, Tsien RY. Measuring calcium signaling using genetically targetable fluorescent indicators. Nat Protoc. 2006; 1:1057–1065. [PubMed: 17406387]

Rau KR, Quinto-Su PA, Hellman AN, Venugopalan V. Pulsed laser microbeam-induced cell lysis: Time-resolved imaging and analysis of hydrodynamic effects. Biophys J. 2006; 91:317–329. [PubMed: 16617076]

Ravin R, Blank PS, Steinkamp A, Rappaport SM, Ravin N, Bezrukov L, Guerrero-Cazares H, Quinones-Hinojosa A, Bezrukov SM, Zimmerberg J. Shear forces during blast, not abrupt changes in pressure alone, generate calcium activity in human brain cells. PLoS One. 2012; 7:e39421. [PubMed: 22768078]

Reichel E, Schmidtkloiber H, Schoffmann H, Dohr G, Eherer A. Interaction of short laser-pulses with biological structures. Opt Laser Technol. 1987; 19:40–44.

Tao W, Wilkinson J, Stanbridge EJ, Berns MW. Direct gene transfer into human cultured cells facilitated by laser micro-puncture of the cell membrane. Proc Natl Acad Sci U S A. 1987; 84:4180–4184. [PubMed: 3473500]

Vogel A, Hentschel W, Holzfuss J, Lauterborn W. Cavitation bubble dynamics and acoustic transient generation in ocular surgery with pulsed neodymium: YAG lasers. Ophthalmology. 1986; 93:1259–1269. [PubMed: 3785885]

Vogel A, Lauterborn W, Timm R. Optical and acoustic investigations of the dynamics of laser-produced cavitation bubbles near a solid boundary. J Fluid Mech. 1989; 206:299–338.

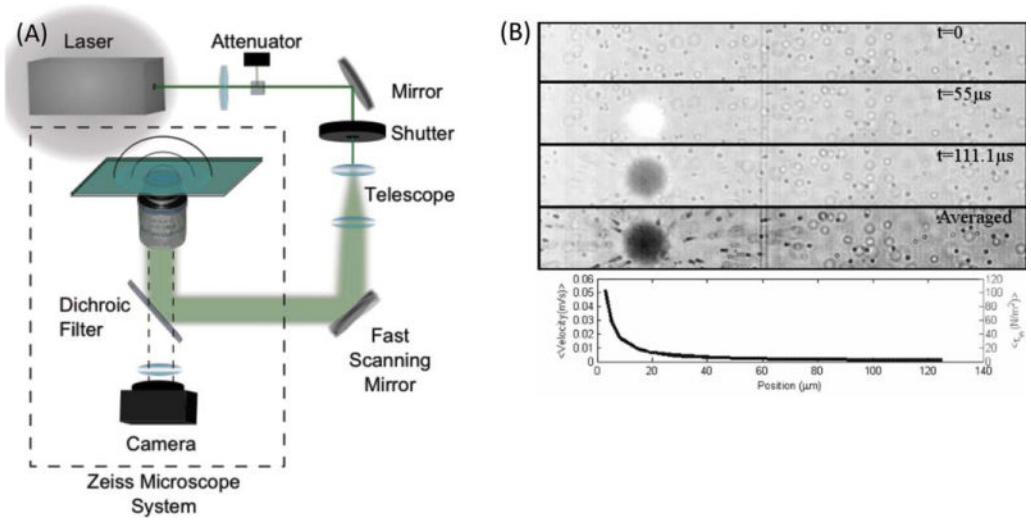

Fig. 1.

Laser setup. (**A**) Coherent Flare 532 nm 100 Hz pulse repetition rate, 2 ns pulse width laser is attenuated by a Glan-Taylor linear polarizer to allow the user to control the laser power entering the microscope. The beam is then directed to a shutter that can gate the laser to allow 1–2 pulses through. A fast scanning mirror is used to steer the laser beam which is focused through a Zeiss 40× 1.3 NA objective. (**B**) Montage showing effect of shockwave at 55 μs intervals. At t = 55 μs the plasma formation is observed. T = 111 ms shows bead displacement near the initiation site. A time averaged position of the beads shows that net displacement occurs more closely to the plasma initiation site. Displaced beads appear as ovals or lines due to movement. A least squares fit of the averaged position of particles is presented. The y-axis is velocity in meters per second and on the x-axis is distance in microns from the initiation site. The particles closer to the initiation site are accelerated rapidly but as the distance from the initiation site increases the velocity drops off quickly. [Color figure can be viewed in the online issue, which is available at wileyonlinelibrary.com.]

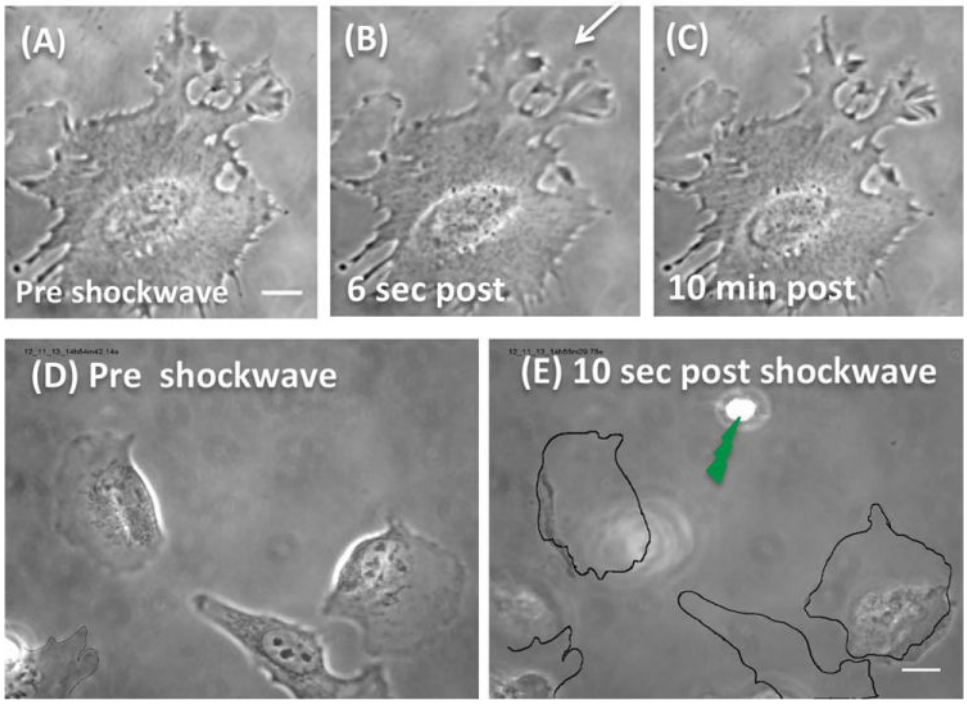

Fig. 2.

(**A**) A magnified phase image of a cell prior to shockwave, scale bar = 10 μm. Thus, the position of the laser is not visible but occurred 70 μm from the cell edge closest to the laser focus spot. (**B**) Six seconds post-shockwave induced with 2.95–4.01 × 10^{12} W/cm^2. The cell appears to have retained its shape and morphology. An arrow depicts the direction from the laser focus spot. (**C**) At 10 minutes, the cell appears unchanged compared to A and B. All cytoplasmic membrane extensions are unchanged in A, B, and C. (**D**) Preshockwave image of a group of cells. (**E**) 10 seconds after a shockwave produced by an irradiance of 43.5 × 10^{12} W/cm^2. Cells are detached and/or rounded-up. [Color figure can be viewed in the online issue, which is available at wileyonlinelibrary.com.]

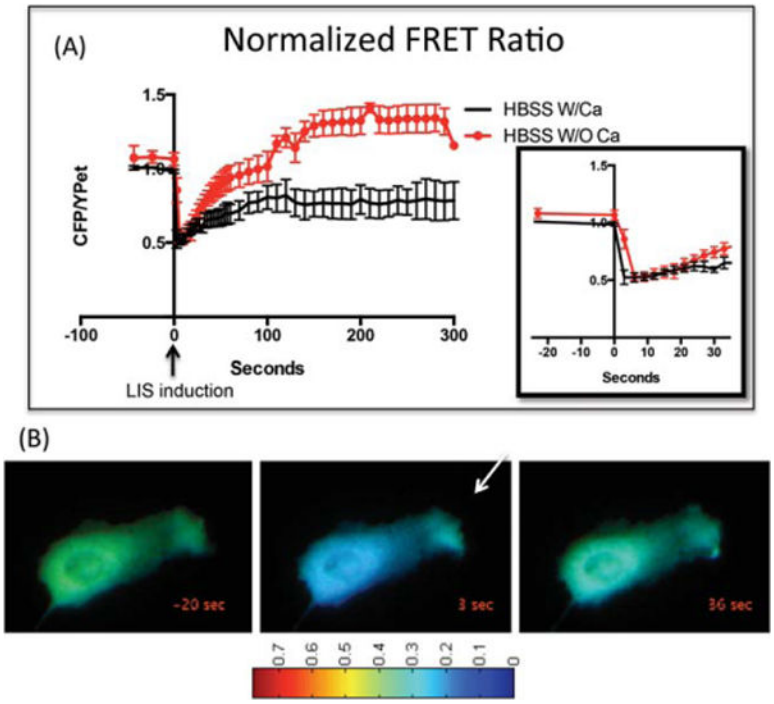

Fig. 3.

(**A**) Normalized FRET ratio plotted as CFP/YPet versus time course of cells in HBSS with (black line) or without calcium (red line). Shockwave was induced at 0 seconds. The FRET ratio depicted is the average taken from the center of the cell. The ratio decreases upon cytoplasmic calcium increase. An inset depicts the FRET ratio from 0 seconds to 30 seconds post-shockwave. (**B**) D3CPV is freely diffusing and therefore the same trends depicted graphically in 3A occur when ratios are measured in other parts of the cell. Ratiometric images show the ratio of 0.35 before (0 seconds), and 0.15 after (3 seconds) shockwave induction. An arrow demonstrates the direction from the shockwave initiation site. Thirty-five seconds post-shock-wave calcium levels are almost the same as preshockwave. This cell has been cropped and magnified to show the respective FRET changes. Thus, laser focus spot point is not shown.